Am J Cancer Res 2025;15(4):1919-1931
www.ajcr.us /ISSN:2156-6976/ajcr0163553

Original Article

PSPH promotes the proliferation and metastasis of esophageal squamous cell carcinoma through MAPK signaling pathways

Mengchu Yao[1*], Yu Xie[2*], Mingde Huang[1], Xiao Han[3], Yu Zhou[1], Mingyue Tao[1], Chang Liu[1], Yongxin Zhao[1], Chengwan Zhang[3], Yong Gao[1]

[1]Department of Oncology, The Affiliated Huai'an No. 1 People's Hospital of Nanjing Medical University, Huai'an 223001, Jiangsu, China; [2]Department of General Surgery, The Affiliated Huai'an No. 1 People's Hospital of Nanjing Medical University, Huai'an 223001, Jiangsu, China; [3]Department of Central Laboratory, The Affiliated Huai'an No. 1 People's Hospital of Nanjing Medical University, Huai'an 223001, Jiangsu, China. [*]Equal contributors.

Received January 24, 2025; Accepted April 17, 2025; Epub April 25, 2025; Published April 30, 2025

Abstract: Esophageal squamous cell carcinoma (ESCC) is an aggressive malignancy with limited therapeutic options and poor prognosis, underscoring the urgent need for novel molecular targets. Here, we identify phosphoserine phosphatase (PSPH) as a key oncogenic driver in ESCC. This study systematically investigated the oncogenic functions of PSPH in ESCC progression and the associated molecular mechanisms. Functional studies revealed that PSPH overexpression markedly enhanced ESCC cell proliferation, migration, and invasion *in vitro*, while PSPH knockdown exerted opposing effects. Mechanistically, transcriptomic and phosphoproteomic analyses identified the mitogen-activated protein kinase (MAPK) pathway as the key downstream effector of PSPH. *In vivo* xenograft studies corroborated these findings, demonstrating that PSPH overexpression markedly promoted tumor growth. Notably, the pharmacological inhibitor of c-Jun N-terminal kinase (JNK) effectively abrogated PSPH-induced tumor progression, unequivocally establishing the MAPK pathway as the dominant mediator of PSPH oncogenic functions. Our findings establish PSPH as a key driver of ESCC progression, promoting migration, proliferation, and invasion via MAPK signaling activation. These results position PSPH as a promising therapeutic target for improving outcomes in patients with ESCC.

Keywords: PSPH, ESCC, MAPK signaling pathway, phosphorylation

Introduction

Esophageal cancer remains a leading gastrointestinal malignancy, ranked as the seventh most common cancer by incidence and sixth by mortality globally, with East Asia bearing the highest disease burden [1]. ESCC and esophageal adenocarcinoma (EAC) represent the two main histological subtypes of esophageal cancer. In China, ESCC accounts for more than 90% of esophageal cancer cases [2-4]. The primary treatment strategy for ESCC involves a multidisciplinary approach that combines surgery, radiotherapy, chemotherapy, targeted therapy, and immunotherapy. However, the five-year survival rate remains below 30%, with most patients experiencing advanced recurrence and metastasis, leading to poor prognoses [5-7]. Although immunotherapy and targeted therapy have modestly improved survival in advanced-stage disease, their efficacy remains limited by resistance and treatment-related toxicities, with only 15-20% of patients achieving durable responses [8, 9]. Consequently, it is crucial to investigate the molecular mechanisms underlying the development and progression of ESCC to enhance prevention, diagnosis, treatment, and prognostic evaluation of esophageal cancer [6, 10].

Emerging evidence highlights the central role of metabolic reprogramming in tumorigenesis. PSPH, a key enzyme in serine phosphorylation metabolism, attracts considerable research interest due to its essential role in catalyzing phosphoserine dephosphorylation, thereby

modulating cellular metabolism, proliferation, and apoptosis [11, 12]. PSPH participates in diverse cellular activities, including proliferation and differentiation, by serving as a biosynthetic precursor for neurotransmitters, phospholipids, glycolipids, purines, and thymidine [13-15]. Deficiency in PSPH is causally associated with congenital neurodevelopmental disorders, including Williams syndrome and neural tube defects, resulting from impaired biosynthesis of essential precursors [16]. Conversely, elevated PSPH expression is associated with several cancers, including cutaneous squamous cell carcinoma, breast cancer, and hepatocellular carcinoma [17-20]. Despite extensive research on PSPH in other tumors, its functional significance in ESCC remains largely unexplored. The MAPK signaling pathway is well-characterized as a central regulator of fundamental cellular processes, including growth, differentiation, and survival. Its dysregulation is mechanistically linked to the pathogenesis of diverse malignancies, particularly ESCC, positioning it as a prime target for therapeutic development [21]. Therefore, systematic elucidation of MAPK-mediated oncogenic mechanisms in ESCC will facilitate the design of novel targeted therapies. In this study, we provide evidence that elevated PSPH expression activates the MAPK pathway to drive tumor progression. These findings demonstrate that PSPH may serve as a potential therapeutic target for ESCC by suppressing MAPK pathway activation. Further investigations are required to evaluate the clinical potential of PSPH-targeted therapies in ESCC treatment.

Material and methods

Source of ESCC patients and tissue specimen collection

We retrospectively collected tumor tissues and matched histologically normal esophageal tissues (≥5 cm from tumor margin) from 192 treatment-naive ESCC patients who underwent radical esophagectomy at the Affiliated Huai'an First People's Hospital of Nanjing Medical University. All cases were staged according to the AJCC 8th edition TNM classification (2020), with histopathological confirmation by two blinded senior pathologists. Immediately after resection, specimens were snap-frozen in liquid nitrogen and stored at -80°C until analysis. This study was approved by the Institutional Review Board of Huai'an First People's Hospital (KY-2024-345-01), and written informed consent was obtained from all participants in accordance with the Declaration of Helsinki.

Cell lines and culture conditions

The human ESCC cell lines (KYSE30, KYSE150, KYSE410, Eca-109, and TE-1) and normal esophageal epithelial cells (HECC) were obtained from the Cell Bank of the Chinese Academy of Sciences (Shanghai, China). Cells were maintained at 37°C in a humidified 5% CO_2 atmosphere in DMEM-high glucose medium (Gibco, USA) supplemented with 10% FBS (Gibco, USA) and 1% penicillin-streptomycin (Gibco, USA), and subcultured at 80-90% confluence every 1-2 days to maintain logarithmic-phase growth.

Animals

Female BALB/c nude mice (age 4-6 weeks) were obtained from GemPharmatech Co., Ltd. (Jiangsu, China) and maintained in individually ventilated cages (IVCs) under specific pathogen-free (SPF) conditions, with ad libitum access to autoclaved water and γ-irradiated feed.

Xenograft tumor model in nude mice

KYSE30 cells were transduced with PSPH-specific shRNA lentiviral vectors (sh-PSPH) or control vectors (sh-Control). Subsequently, 5×10^6 lentivirus-transduced KYSE30 cells in 100 μL PBS were subcutaneously injected into the left flank of female BALB/c nude mice (age 4-6 weeks, n=5 per group). Mice were housed under specific pathogen-free (SPF) conditions with daily monitoring of xenograft tumor growth. Tumor volumes were calculated every 5 days using the formula: V (mm^3) = [length (mm) × width^2 (mm^2)]/2. After a 3-week observation period, mice were placed in a pre-charged euthanasia chamber (≤20 mice per batch) and exposed to compressed CO_2 at a flow rate of 20% chamber volume displacement per minute (5.8 L/min for standard chambers). The flow rate was maintained to ensure rapid unconsciousness (typically <30 sec) followed by respiratory arrest. Death was confirmed by the absence of pedal reflex, fixed dilated pupils, and cessation of breathing for ≥3 minutes. The xenograft tumors were dissected and weighed, with a portion of the tumor tissue collected for

immunohistochemical analysis. All animal experiments were approved by the Animal Care and Use Committee of Huai'an First People's Hospital, affiliated with Nanjing Medical University (Approval No. DW-P-2024-023-01).

Lentiviral infection

The lentiviruses for PSPH overexpression and knockdown were produced by GeneChem (Shanghai, China). Lentiviral infection was performed according to the manufacturer's instructions. Cells were infected at a multiplicity of infection (MOI) of 10 for 16 hours with 10 μg/mL polybrene (Sigma, Germany). Subsequently, the infected cells were selected using 5 μg/mL puromycin.

Western blotting

ESCC cells were lysed in neutral lysis buffer (VICMED, China) containing protease and phosphatase inhibitors, centrifuged at 12,000 ×g for 20 min, and the supernatant was collected. The protein concentration was measured by BCA assay (NCM, China). Proteins were separated by SDS-PAGE, transferred to PVDF membranes (ROCHE, Switzerland), blocked with 5% non-fat milk, and probed with primary antibodies (4°C, overnight) followed by secondary antibodies. Protein bands were visualized using a ChemiDoc™ XRS+ system (Bio-Rad, USA) and analyzed with Image Lab software. Vinculin served as the loading control.

Quantitative real-time PCR (qRT-PCR)

Total RNA was extracted from patient tissues using an NcmSpin Cell/Tissue Total RNA Kit (NCM, China) and reverse transcribed into cDNA using a FastQuant RT Kit (Tiangen, China) according to the manufacturers' instructions. qPCR was performed with SYBR Green qPCR Master Mix (MCE, USA) on a real-time PCR detection system (Thermo Fisher Scientific, USA). The PSPH-specific primers were as follows: forward primer, 5'-GAGGACGCGGTGTCAGAAAT-3'; reverse primer, 5'-GAGGACGCGGTGTCAGAAAT-3'. The GAPDH primers were: forward, 5'-ACCAGCCTCCAAGATCAGC-3'; reverse, 5'-TGCTAAGCGTTGGTGGTGC-3'. Each sample was analyzed in triplicate, and relative expression levels were calculated using the $2^{-\Delta\Delta Ct}$ method.

CCK8 assay

ESCC cells were seeded at a density of 2×10^3 cells per well in 96-well plates. Cell viability was assessed at 0, 24, 48, 72, and 96 h using the Cell Counting Kit-8 (CCK-8; VICMED, China). Absorbance was measured at 450 nm using a microplate reader (Hidex, Finland).

Colony formation assay

ESCC cells were seeded in 6-well plates at a density of 800 cells per well and cultured with regular medium replacement. After 2 weeks of culture, the formed colonies were fixed with 4% formaldehyde and stained with 0.1% crystal violet following standard protocols.

Transwell assay

Cell migration ability was assessed using transwell chambers (8 μm pore size; Corning, USA). A total of 3×10^4 cells suspended in 200 μL serum-free DMEM, with or without Matrigel (BD Biosciences, USA), were seeded in the upper chamber. The lower chamber contained DMEM supplemented with 10% FBS as a chemoattractant. After 48 h incubation at 37°C with 5% CO_2, the membrane was fixed with 4% paraformaldehyde and stained with 0.1% crystal violet. Migrated cells on the underside of the membrane were imaged and counted using an inverted microscope (Zeiss, Germany).

Cell scratch assay

ESCC cells were seeded in 6-well plates and cultured until reaching 90% confluency. After gently removing the culture medium, a linear wound was created in the confluent cell monolayer using a sterile pipette tip. The cells were then washed twice with PBS to remove detached cellular debris. After washing twice with PBS to remove cellular debris, wound areas were imaged at 0 and 48 h post-wounding using an inverted microscope (Zeiss, Germany).

SP600125 treatment

For *in vitro* experiment, ESCC cells were treated with 20 μM SP600125 (MCE, USA) or an equal volume of 0.1% DMSO (vehicle control) for 48 h.

RNA-seq analysis and Gene Ontology enrichment analysis

Total RNA was extracted from PSPH-knockdown and control KYSE30 cells using the RNeasy Kit (Qiagen, Germany) according to the protocol of manufacturer. First-strand cDNA was synthe-

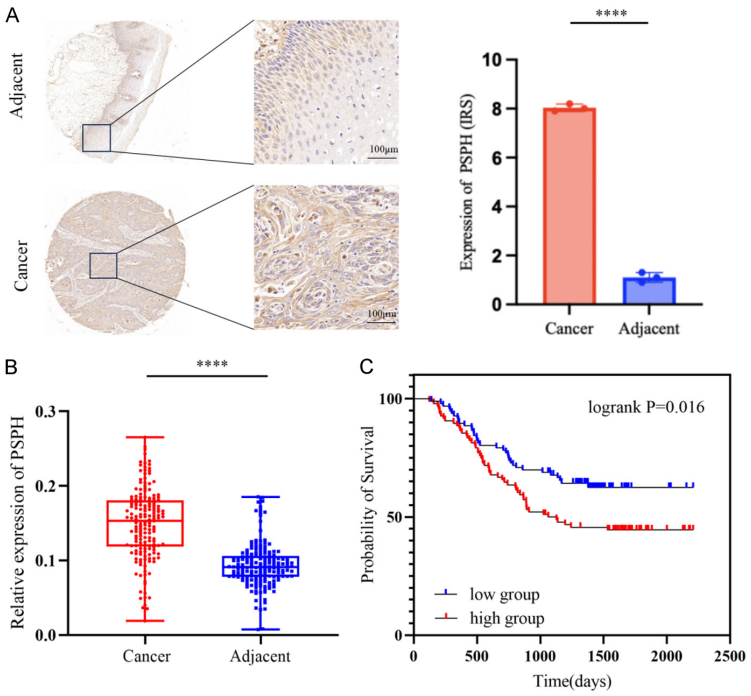

Figure 1. PSPH is overexpressed in ESCC patient tissues with poor prognosis. A. PSPH protein levels in ESCC tissues and the adjacent tissues was detected by immunohistochemical staining evaluated by immunoreactive Score (IRS). Scale bar represents 200 μm. Paired twotailed Student's t-test. ****P<0.0001. B. PSPH mRNA expression levels in ESCC and paired adjacent tissues (n=192) were quantified using qRT-PCR. Paired twotailed Student's t-test. ****P<0.0001. C. Based on PSPH mRNA expression levels, the 192 samples were stratified into high-expression (n=81) and low-expression (n=81) groups using the median value. Kaplan-Meier (KM) curves with log-rank tests. P=0.016.

sized with random hexamer primers and M-MuLV Reverse Transcriptase (RNase H^-). Second-strand cDNA synthesis was then performed using DNA Polymerase I and RNase H. The libraries were sequenced on an Illumina NovaSeq 6000 platform. Differential expression analysis between groups was conducted with the ballgown R package, with adjusted *P*-values calculated via the Benjamini-Hochberg method to control the false discovery rate (FDR). Genes showing adjusted *P*-values <0.05 were considered differentially expressed. Functional enrichment analysis was performed using the clusterProfiler R package to identify significantly enriched Gene Ontology (GO) terms and Kyoto Encyclopedia of Genes and Genomes (KEGG) pathways.

Co-Immunoprecipitation (Co-IP)

Cells were lysed in IP lysis buffer (NCM, China) supplemented with EDTA-free protease inhibitor cocktail and 1 mM PMSF. Clarified lysates (equivalent to 1×10^7 cells) were incubated overnight at 4°C with anti-MEK or anti-PSPH antibodies precoupled to Protein A/G magnetic beads (MCE, USA). After three washes with lysis buffer, immunoprecipitates were denatured and separated by SDS-PAGE, followed by immunoblotting with the appropriate antibodies.

Statistical analysis

Data normality was assessed using the Shapiro-Wilk test, while homogeneity of variance was evaluated with Levene's test. For normally distributed data, two-group comparisons were performed using paired or unpaired Student's t-tests. Multigroup comparisons were analyzed by one-way ANOVA followed by Tukey's post hoc test. Data are expressed as mean± SD. Survival analyses were conducted using Kaplan-Meier (KM) curves with log-rank tests. Data visualization and statistical analysis were conducted using GraphPad Prism 9.0. P<0.05 was considered to indicate statistical significance.

Results

PSPH is upregulated in ESCC with poor prognosis

To investigate PSPH expression in ESCC tissues, we constructed a tissue microarray comprising 192 ESCC samples with paired adjacent normal tissues. PSPH protein levels were evaluated by immunohistochemistry (IHC) using the IRS scoring system, revealing predominant localization in the cell membrane and cytoplasm. Notably, PSPH expression was significantly upregulated in tumor tissues compared to normal counterparts (**Figure 1A**). Consistent with protein data, qPCR analysis demonstrated significantly higher PSPH mRNA levels in tumor tissues (**Figure 1B**). Kaplan-Meier survival analysis of the 192 patients cohort stratified by

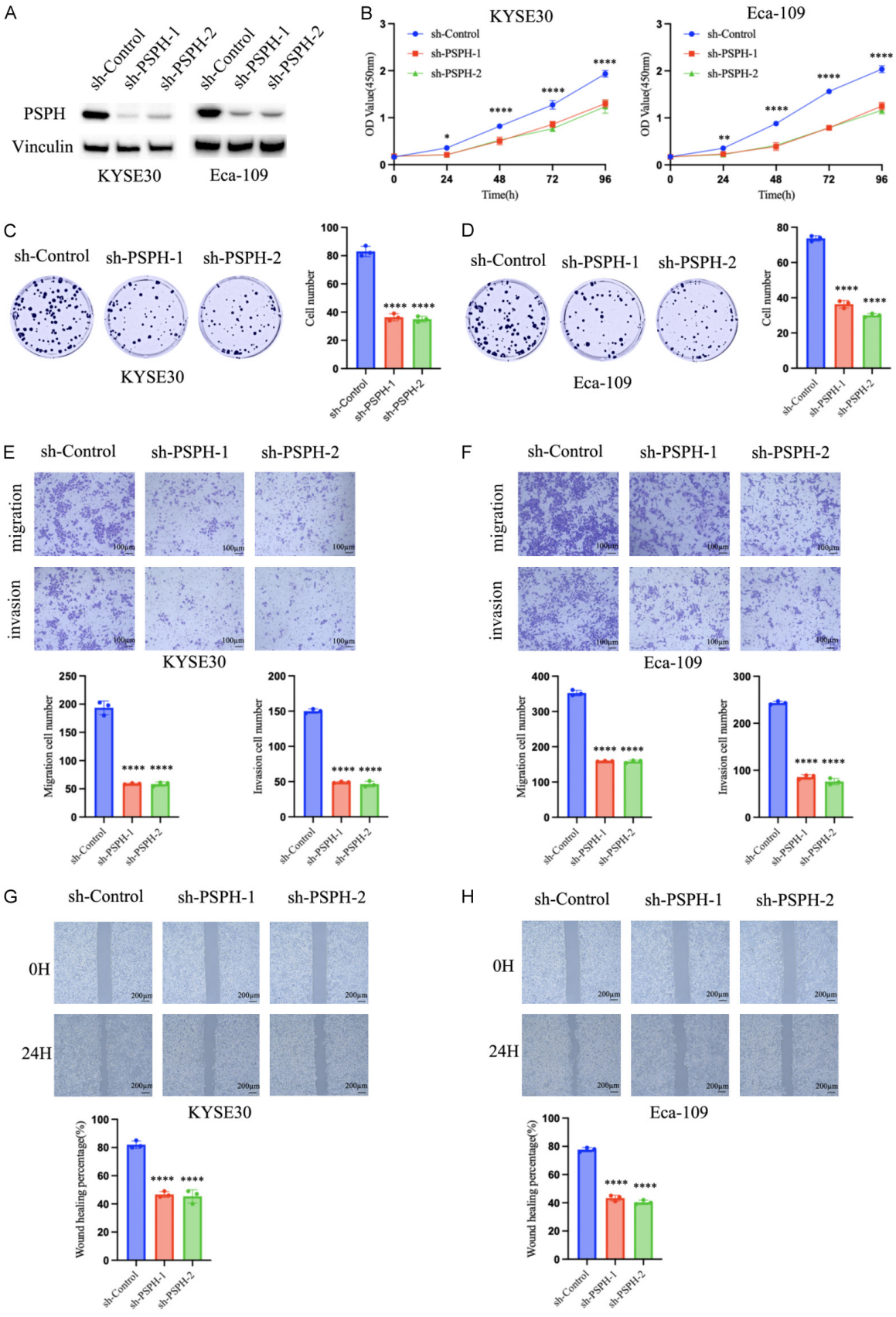
A
sh-Control
sh-PSPH-1
sh-PSPH-2
sh-Control
sh-PSPH-1
sh-PSPH-2
PSPH
Vinculin
KYSE30
Eca-109
B
KYSE30
Eca-109
sh-Control
sh-PSPH-1
sh-PSPH-2
OD Value(450nm)
Time(h)
C
sh-Control
sh-PSPH-1
sh-PSPH-2
KYSE30
Cell number
D
sh-Control
sh-PSPH-1
sh-PSPH-2
Eca-109
Cell number
E
sh-Control
sh-PSPH-1
sh-PSPH-2
migration
invasion
KYSE30
Migration cell number
Invasion cell number
F
sh-Control
sh-PSPH-1
sh-PSPH-2
migration
invasion
Eca-109
Migration cell number
Invasion cell number
G
sh-Control
sh-PSPH-1
sh-PSPH-2
0H
24H
KYSE30
Wound healing percentage(%)
H
sh-Control
sh-PSPH-1
sh-PSPH-2
0H
24H
Eca-109
Wound healing percentage(%)

Figure 2. Knockdown of PSPH inhibits ESCC cell proliferation, invasion and metastasis. (A) Western blot analysis of PSPH knockdown by sh-PSPH-1/2 in KYSE30 and Eca-109 cells. (B) CCK-8 proliferation assay in ESCC cells after PSPH knockdown (n=3). One-way ANOVA. *P<0.05, **P<0.01, ****P<0.0001. (C, D) Colony formation of KYSE30 (C) and Eca-109 (D) cells after PSPH knockdown (n=3). One-way ANOVA. ****P<0.0001. (E, F) The effect of PSPH knockdown on the invasiveness of KYSE30 (E) and Eca-109 (F) cells (n=3). Scale bar: 100 μm. One-way ANOVA. ****P<0.0001. (G, H) Wound healing assay of KYSE30 (G) and Eca-109 (H) cells after PSPH knockdown (n=3). Scale bar: 200 μm. One-way ANOVA. ****P<0.0001.

PSPH expression (high vs low) showed that elevated PSPH expression correlated with reduced overall survival (**Figure 1C**).

PSPH enhances the migration, proliferation and invasion of ESCC cells

The expression of PSPH was assessed by western blot analysis in various esophageal cancer cell lines, enabling identification of cell lines with relatively high and low expression levels (Figure S1A). To investigate the epigenetic function of PSPH in ESCC, we generated PSPH-knockdown KYSE30 and Eca-109 cells using shRNA-PSPH lentivirus, with transfection efficiency confirmed by western blotting (**Figure 2A**). Cellular assays demonstrated that PSPH knockdown significantly inhibited proliferation (**Figure 2B-D**), migration, and invasion (**Figure 2E-H**) of ESCC cells. For PSPH overexpression, Ubi-MCS-Puro-3FLAG-PSPH was transfected into KYSE410 and TE1 cells (**Figure 3A**). Elevated PSPH expression increased cell growth rates (**Figure 3B**, **3C**) and enhanced invasion and migration capacities (**Figure 3D-G**).

PSPH activates the MAPK signaling pathway through MEK interaction in ESCC

To elucidate the molecular mechanisms underlying PSPH-mediated ESCC progression, we performed RNA-seq on PSPH-knockdown and control KYSE30 cells. Differential expression analysis identified 445 downregulated and 1,121 upregulated genes (**Figure 4A**). Gene Ontology (GO) enrichment analysis revealed PSPH association with biological processes including cellular processes and biological regulation, as well as molecular functions such as binding and catalytic activity (**Figure 4B**). KEGG pathway analysis demonstrated PSPH potential involvement in cancer-related pathways, particularly the MAPK signaling pathway (**Figure 4C**). Western blotting showed that PSPH knockdown reduced phosphorylation levels of MEK, JNK, and p38, whereas PSPH overexpression enhanced phosphorylation of these proteins (**Figure 4D**, **4E**). To investigate how PSPH directly regulates MAPK phosphorylation, we selected KYSE410 ESCC cells with high endogenous PSPH expression. Proteins were immunoprecipitated using anti-PSPH antibody, followed by western blotting to analyze MAPK pathway components. The Co-IP results confirmed a physical interaction between PSPH and MEK (**Figure 4F**). Reciprocally, reverse Co-IP using anti-MEK antibody further validated this interaction. These findings demonstrate that PSPH promotes MAPK signaling activation and ESCC progression through direct binding to MEK, thereby enhancing phosphorylation of downstream effectors.

PSPH promotes ESCC tumor growth in vivo

To investigate the role of PSPH in ESCC tumor progression *in vivo*, we established xenograft models by subcutaneously injecting control or PSPH-knockdown KYSE30 cells into nude mice (**Figure 5A**). Tumor growth analysis revealed significantly reduced growth rates in PSPH-knockdown tumors compared to controls (**Figure 5B-D**). For histopathological evaluation, formalin-fixed paraffin-embedded (FFPE) tumor sections were stained with antibodies against PSPH, p-MEK (S217/221), p-JNK (T183/Y185), and p-P38 (T180/Y182). Immunohistochemistry demonstrated markedly decreased phosphorylation levels of MEK, JNK, and p38 in PSPH-knockdown tumors (**Figure 5E**). These results substantiate that PSPH promotes ESCC tumor growth *in vivo* through MAPK pathway activation.

The PSPH-promoted migration, proliferation, and invasion of ESCC cells are reversed by the JNK inhibitor SP600125

To definitively determine PSPH regulatory effect on the MAPK pathway, we pretreated PSPH-overexpressing TE1 and KYSE410 cells with the JNK inhibitor SP600125 (20 μM, 48 h). Western blotting showed that SP600125 could reverse the increase in p-MEK, p-JNK, and p-P38

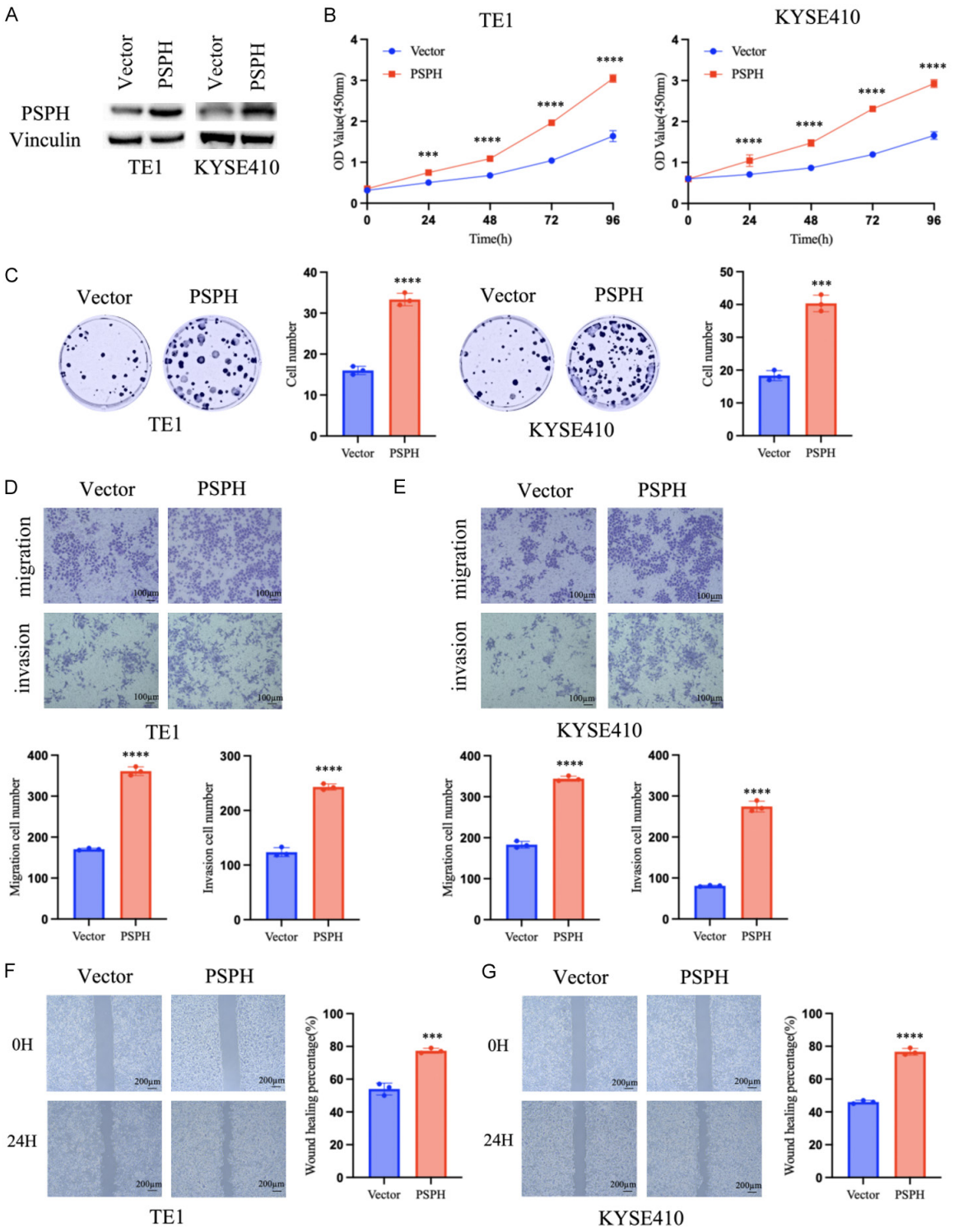

Figure 3. Overexpression of PSPH promotes proliferation, invasion and metastasis of ESCC cells. (A) Western blot analysis of PSPH overexpression in TE1 and KYSE410 cells by plasmid transfection. (B) CCK-8 proliferation assay in ESCC cells after PSPH overexpression (n=3). Unpaired two-tailed Student's t-test. ***P<0.001, ****P<0.0001. (C) Colony formation of ESCC cells after PSPH overexpression (n=3). Unpaired two-tailed Student's t-test. ***P<0.001, ****P<0.0001. (D, E) The effect of PSPH overexpression on the invasiveness of TE1 (D) and KYSE410 (E) cells (n=3). Scale bar: 100 μm. Unpaired two-tailed Student's t-test. ****P<0.0001. (F, G) Wound healing assay of TE1 (F) and KYSE410 (G) cells after PSPH overexpression (n=3). Scale bar: 200 μm. Unpaired two-tailed Student's t-test. ***P<0.001, ****P<0.0001.

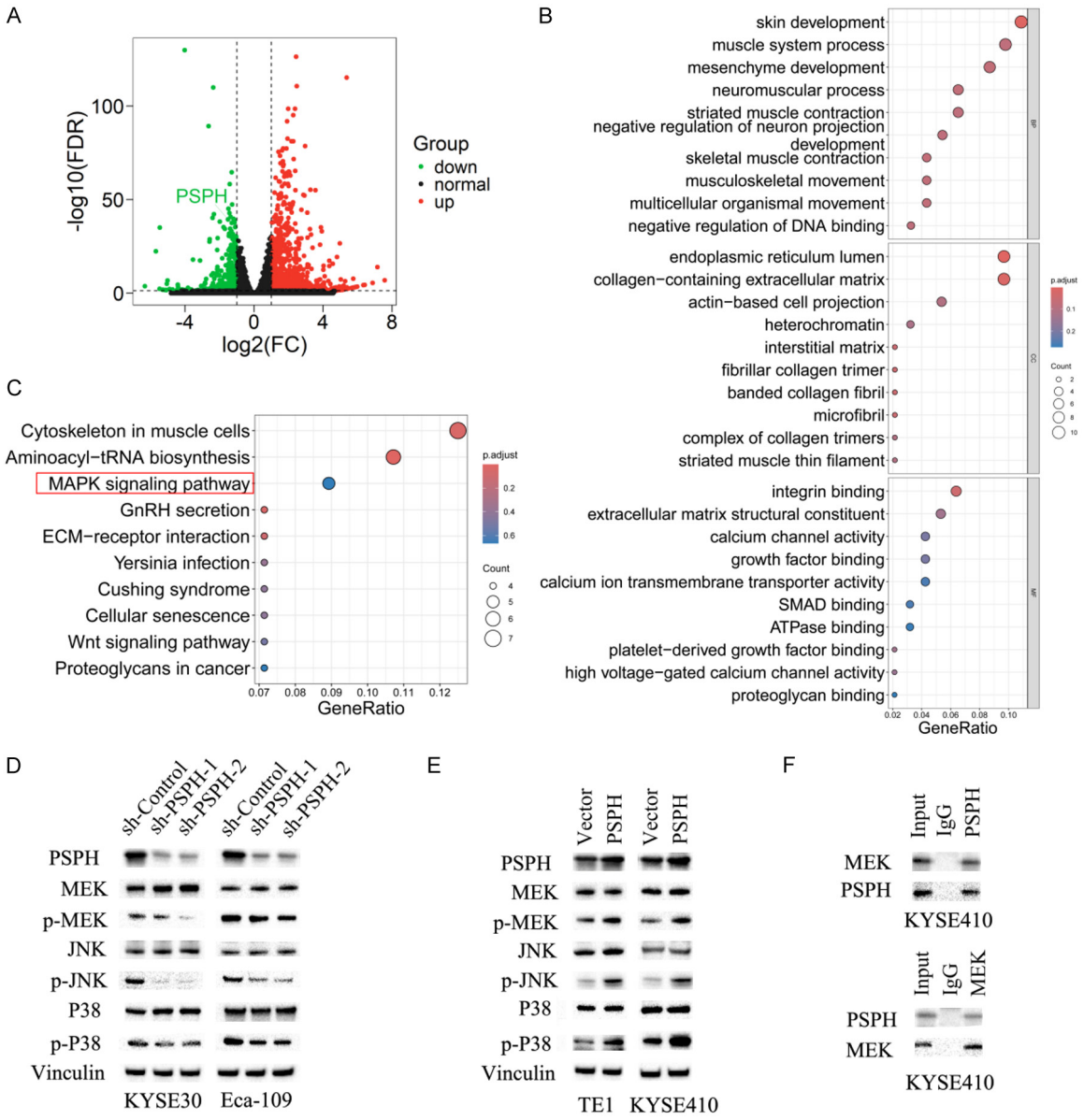

Figure 4. PSPH regulates the MAPK signaling pathways through MEK interaction in ESCC. Transcriptomic profiles of KYSE30 cells with PSPH knockdown and control groups were analyzed by RNA-seq (three biological replicates per group). A. Volcano plot of differentially expressed genes (DEGs) between PSPH-knockdown and control groups. B. GO classification enrichment analysis. C. Enrichment analysis of KEGG pathways. D. Western blot analysis of MAPK pathway proteins in KYSE30 and Eca109 cells after PSPH knockdown. E. Western blot analysis of MAPK pathway proteins in TE1 and KYSE410 cells after PSPH overexpression. F. Co-immunoprecipitation (Co-IP) analysis of PSPH-MEK interaction in KYSE410 cells.

expression induced by PSPH overexpression (**Figure 6A**). Functional assays further demonstrated that SP600125 attenuated PSPH-promoted oncogenic phenotypes, including enhanced cell proliferation (**Figure 6B**) and invasion (**Figure 6C**, **6D**), with consistent results observed in both cell lines (Figure S1B-S1D). These findings establish that PSPH promotes ESCC malignancy through MAPK pathway activation.

Discussion

ESCC continues to pose a substantial global health burden, especially in high-incidence regions such as East Asia [22, 23]. Current

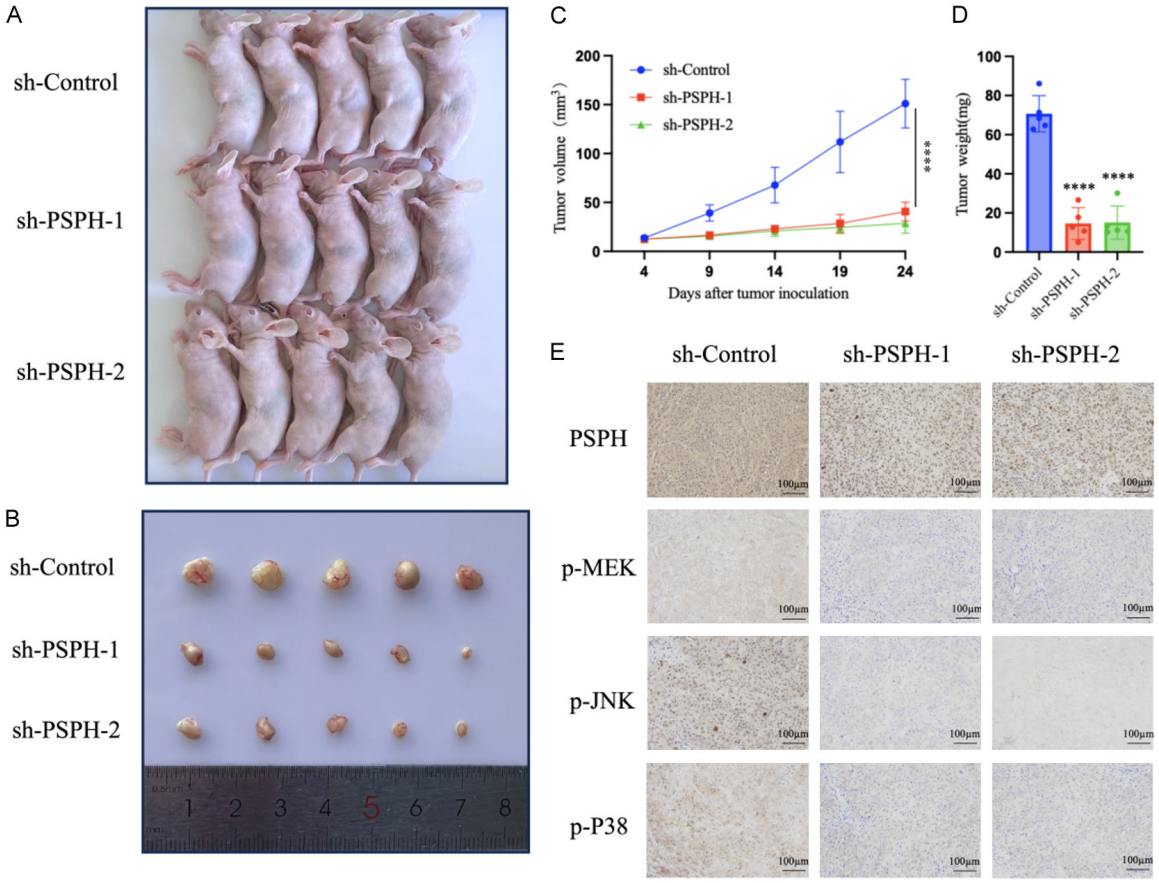

Figure 5. PSPH knockdown suppressed ESCC tumor growth via MAPK pathway *in vivo*. (A-D) Compared with the control group, the subcutaneous tumors formed by KYSE30 cells with PSPH knockdown exhibited significantly smaller size (A, B), lower tumor volume (C), and reduced growth rate (D). One-way ANOVA. *P<0.05, ****P<0.0001. (E) Immunohistochemical staining of PSPH and MAPK pathway markers (p-MEK, p-JNK, p-P38) in xenograft tumor tissues. Scale bar: 100 μm.

treatment approaches primarily include surgical resection, radiotherapy, and chemotherapy, often used in combination. Despite advancements in these methods, the prognosis for patients with advanced ESCC remains poor. Therefore, there is an urgent need to identify metastatic factors and to gain a deeper understanding of the molecular mechanisms underlying ESCC [24, 25]. Previous studies on PSPH have revealed its critical role in various biological processes, particularly in serine metabolism and its significance in cancer biology [26]. Serine, a non-essential amino acid, is synthesized from the glycolytic intermediate 3-phosphoglycerate through a three-step enzymatic cascade involving phosphoglycerate dehydrogenase (PHGDH), phosphoserine aminotransferase (PSAT1), and PSPH. As one of the most frequent phosphorylation sites in proteins, serine exhibits upregulated biosynthesis in multiple cancers, where it fuels tumor growth by supporting nucleotide and amino acid production [27, 28]. Notably, cancer cells upregulate PSPH-mediated serine synthesis to meet their heightened metabolic demands [29]. Emerging evidence suggests that L-serine synthesis acts as a metabolic checkpoint regulating cell cycle progression via MAPK pathway activation [30]. Ross et al. reported that the MAPK cascade is activated inducing serine biosynthesis in metastatic melanoma cells [31]. These studies indicate that the biological function of PSPH is related to serine phosphorylation. Emerging evidence has demonstrated that PSPH overexpression in multiple malignancies serves as both a prognostic biomarker and therapeutic target in advanced hepatocellular carcinoma, cutaneous squamous cell carcinoma, and

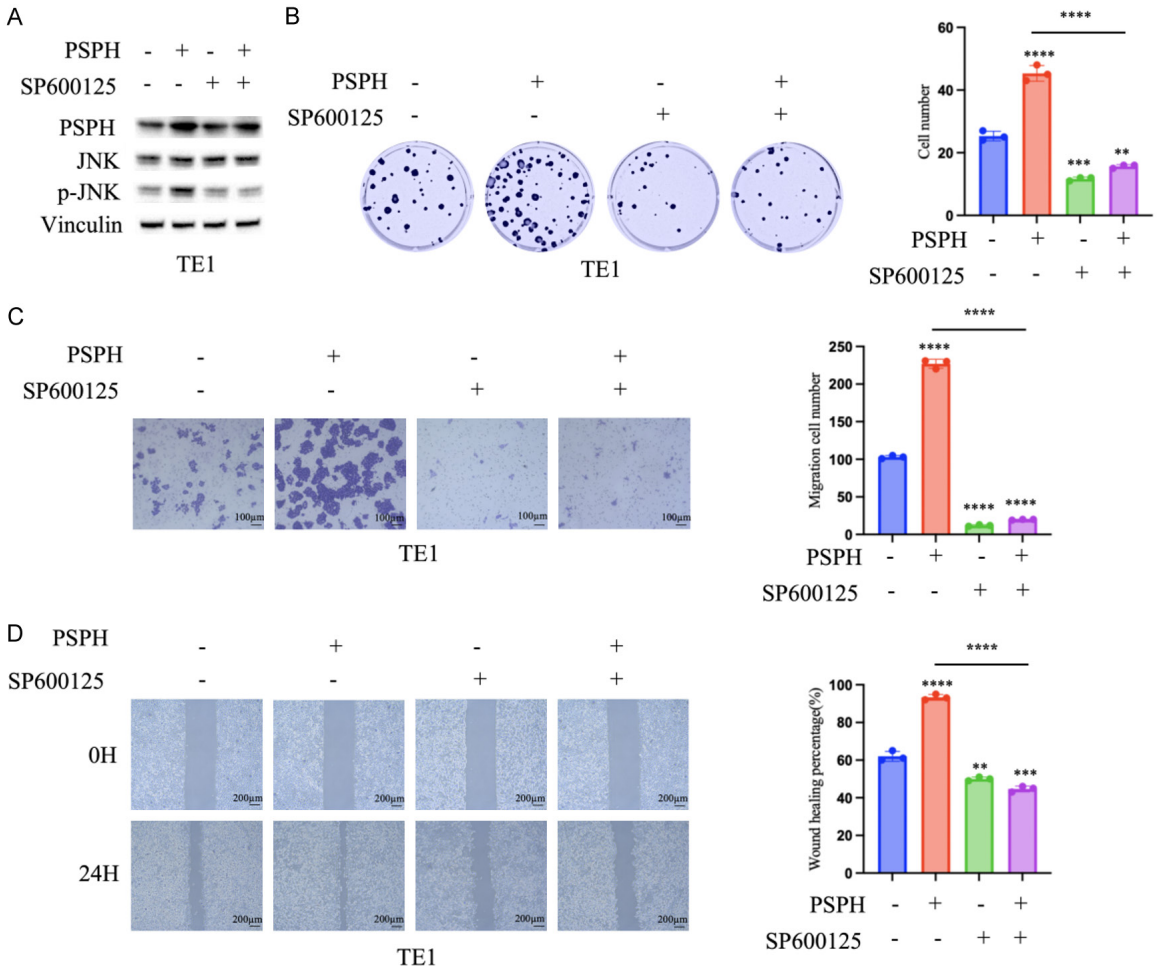

Figure 6. SP600125 blocks PSPH-mediated oncogenic effects. A. Western blot analysis of p-JNK in TE1 cells with PSPH overexpression treated with or without SP600125. B. Colony formation of TE1 cells with PSPH overexpression treated with or without SP600125 (n=3). One-way ANOVA. **P<0.01, ***P<0.001, ****P<0.0001. C. Migration assays in TE1 cells with PSPH overexpression treated with or without SP600125 (n=3). Scale bar: 100 μm. One-way ANOVA. ****P<0.0001. D. Wound healing assay of TE1 cells with PSPH overexpression treated with or without SP600125 (n=3). Scale bar: 200 μm. One-way ANOVA. **P<0.01, ***P<0.001, ****P<0.0001.

colorectal cancer, with PSPH inhibition shown to enhance 5-fluorouracil sensitivity in colorectal cancer models [19, 20, 32], highlighting its dual potential as a diagnostic marker for tumor aggressiveness and a druggable target for combination therapies.

This study elucidated a clinically significant relationship between PSPH expression and aggressive ESCC phenotypes, demonstrating that elevated PSPH levels strongly correlate with poor patient prognosis, suggesting its critical role in modulating ESCC malignancy. This correlation highlighted the potential of PSPH as a biomarker for aggressive disease, which could aid in stratifying patients based on their risk profiles. Specifically, our investigations revealed that PSPH significantly enhanced cellular migration, proliferation, and invasion - hallmark features commonly associated with aggressive tumors. The ability of cancer cells to migrate and invade surrounding tissues is a key factor that contributes to the poor outcomes observed in patients with high PSPH expression. Furthermore, we explored the mechanistic pathways through which PSPH exerts its influence. The activation of the MAPK signaling pathway by PSPH provided additional insights into its role in driving the aggressive behavior of ESCC cells. The MAPK pathway is well-known for its involvement in critical processes such as cell growth, differentiation, and survival [33-

35]. The MAPK pathway consists of a series of protein kinases that transmit signals from the cell surface to the nucleus, thereby activating transcription factors that regulate gene expression [36, 37]. Key components of this pathway include MEK, JNK, and P38 [38]. Recent studies have shown that the MAPK pathway is involved not only in normal cellular functions but also plays a crucial role in pathological conditions, particularly in cancers [39-41]. Dysregulation of MAPK signaling is associated with various types of tumors, promoting cell proliferation, survival, and metastasis [42, 43]. For instance, PSPH promotes the metastasis and proliferation of non-small cell lung cancer through the MAPK signaling pathway [17]. We demonstrated that PSPH enhances MAPK component phosphorylation, activating downstream effectors to drive tumorigenesis. This suggests that PSPH regulates the expression or activity of MAPK pathway molecules, thus promoting ESCC cell proliferation and survival. Furthermore, PSPH promotes tumor growth *in vivo*, reinforcing its role as a key regulator of the ESCC phenotype. Inhibition of PSPH significantly reduced tumor growth in our experiments, highlighting its critical function in tumor biology.

Inhibitors targeting specific MAPK pathway components are being actively explored in clinical settings to enhance therapeutic efficacy and overcome resistance in cancer treatment [44]. As our understanding of the MAPK pathway role in tumor progression, researchers are developing inhibitors targeting key kinases such as MEK, JNK, and p38 [45]. These inhibitors disrupt the hyperactivated MAPK pathway in cancer cells, thus suppressing tumor proliferation, survival, and metastasis [46, 47]. Recent clinical trials indicated that some JNK inhibitors exhibited antitumor activity in cancers like melanoma and colorectal cancer [48-50]. These inhibitors significantly reduced tumor growth rates and elicited sustained responses in some patients. Furthermore, studies demonstrated that combining MAPK inhibitors with immunotherapy or chemotherapy enhanced therapeutic efficacy and overcomes tumor resistance [51]. Interestingly, we found that JNK inhibitors reversed PSPH-induced tumor growth, highlighting a potential therapeutic avenue. These findings open new possibilities for therapies targeting PSPH-mediated signaling pathways, potentially mitigating the aggressive phenotype of high-PSPH ESCC. The limitation of this study lies in its exclusive focus on a single cancer type (ESCC), which may limit the generalizability of the findings to other cancers. Future studies in other cancer types and pathway mechanisms are needed to fully elucidate PSPH's role in tumor biology.

In summary, the tumor-promoting factor PSPH is highly expressed in cancer tissues and significantly contributes to ESCC progression. This study provides the first evidence that PSPH promotes ESCC growth through MAPK pathway activation. Our findings support the potential of PSPH as a therapeutic target for inhibiting the development of esophageal cancer and as an independent prognostic marker that could be useful for patient survival.

Acknowledgements

This work was supported by the Huai'an Health and Science Research Project (HAWJ2024004) and the Foundation of Science and technology development Program of Nanjing Medical University (NMUB20230107).

Disclosure of conflict of interest

None.

Address correspondence to: Dr. Yong Gao, Department of Oncology, The Affiliated Huai'an No. 1 People's Hospital of Nanjing Medical University, #1 Huanghe Road, Huai'an 223000, Jiangsu, China. Tel: +86-13852388860; E-mail: hayygaoy@njmu.edu.cn; Dr. Chengwan Zhang, Department of Central Laboratory, The Affiliated Huai'an No. 1 People's Hospital of Nanjing Medical University, #1 Huanghe Road, Huai'an 223000, Jiangsu, China. Tel: +86-15851762048; E-mail: hayyzhchw@njmu.edu.cn

References

[1] Sung H, Ferlay J, Siegel RL, Laversanne M, Soerjomataram I, Jemal A and Bray F. Global cancer statistics 2020: GLOBOCAN estimates of incidence and mortality worldwide for 36 cancers in 185 countries. CA Cancer J Clin 2021; 71: 209-249.

[2] Xia C, Dong X, Li H, Cao M, Sun D, He S, Yang F, Yan X, Zhang S, Li N and Chen W. Cancer statistics in China and United States, 2022: profiles, trends, and determinants. Chin Med J (Engl) 2022; 135: 584-590.

[3] Huang FL and Yu SJ. Esophageal cancer: risk factors, genetic association, and treatment. Asian J Surg 2018; 41: 210-215.
[4] Agrawal N, Jiao Y, Bettegowda C, Hutfless SM, Wang Y, David S, Cheng Y, Twaddell WS, Latt NL, Shin EJ, Wang LD, Wang L, Yang W, Velculescu VE, Vogelstein B, Papadopoulos N, Kinzler KW and Meltzer SJ. Comparative genomic analysis of esophageal adenocarcinoma and squamous cell carcinoma. Cancer Discov 2012; 2: 899-905.
[5] Borggreve AS, Kingma BF, Domrachev SA, Koshkin MA, Ruurda JP, van Hillegersberg R, Takeda FR and Goense L. Surgical treatment of esophageal cancer in the era of multimodality management. Ann N Y Acad Sci 2018; 1434: 192-209.
[6] Zhu H, Ma X, Ye T, Wang H, Wang Z, Liu Q and Zhao K. Esophageal cancer in China: practice and research in the new era. Int J Cancer 2023; 152: 1741-1751.
[7] Li R, Huang B, Tian H and Sun Z. Immune evasion in esophageal squamous cell cancer: from the perspective of tumor microenvironment. Front Oncol 2022; 12: 1096717.
[8] Alsina M, Moehler M and Lorenzen S. Immunotherapy of esophageal cancer: current status, many trials and innovative strategies. Oncol Res Treat 2018; 41: 266-271.
[9] Onaitis M. Commentary: induction immunotherapy for esophageal cancer: a safe start. J Thorac Cardiovasc Surg 2021; 161: 844.
[10] Dinh HQ, Pan F, Wang G, Huang QF, Olingy CE, Wu ZY, Wang SH, Xu X, Xu XE, He JZ, Yang Q, Orsulic S, Haro M, Li LY, Huang GW, Breunig JJ, Koeffler HP, Hedrick CC, Xu LY, Lin DC and Li EM. Integrated single-cell transcriptome analysis reveals heterogeneity of esophageal squamous cell carcinoma microenvironment. Nat Commun 2021; 12: 7335.
[11] Rawat V, Malvi P, Della Manna D, Yang ES, Bugide S, Zhang X, Gupta R and Wajapeyee N. PSPH promotes melanoma growth and metastasis by metabolic deregulation-mediated transcriptional activation of NR4A1. Oncogene 2021; 40: 2448-2462.
[12] Peng ZP, Liu XC, Ruan YH, Jiang D, Huang AQ, Ning WR, Jiang ZZ, Zheng L and Wu Y. Downregulation of phosphoserine phosphatase potentiates tumor immune environments to enhance immune checkpoint blockade therapy. J Immunother Cancer 2023; 11: e005986.
[13] Wang T, Zhou LY, Li XM, Liu F, Liang L, Chen XZ, Ju J, Ponnusamy M, Wang K, Liu CY, Yan KW and Wang K. ABRO1 arrests cardiomyocyte proliferation and myocardial repair by suppressing PSPH. Mol Ther 2023; 31: 847-865.
[14] Ma H, He S, Li Y, Zhang X, Chang H, Du M, Yan C, Jiang S, Gao H, Zhao J and Wang Q. Augmented mitochondrial transfer involved in astrocytic PSPH attenuates cognitive dysfunction in db/db mice. Mol Neurobiol 2024; 61: 8872-8885.
[15] Wang J, Xie GF, He Y, Deng L, Long YK, Yang XH, Ma JJ, Gong R, Cen WJ, Ye ZL, Zeng YX, Wang HY and Shao JY. Interfering expression of chimeric transcript SEPT7P2-PSPH promotes cell proliferation in patients with nasopharyngeal carcinoma. J Oncol 2019; 2019: 1654724.
[16] Tabatabaie L, Klomp LW, Berger R and de Koning TJ. L-serine synthesis in the central nervous system: a review on serine deficiency disorders. Mol Genet Metab 2010; 99: 256-262.
[17] Liao L, Ge M, Zhan Q, Huang R, Ji X, Liang X and Zhou X. PSPH mediates the metastasis and proliferation of non-small cell lung cancer through MAPK signaling pathways. Int J Biol Sci 2019; 15: 183-194.
[18] Park SH, Ju JS, Woo H, Yun HJ, Lee SB, Kim SH, Győrffy B, Kim EJ, Kim H, Han HD, Eyun SI, Lee JH and Park YY. The m(6)A writer RBM15 drives the growth of triple-negative breast cancer cells through the stimulation of serine and glycine metabolism. Exp Mol Med 2024; 56: 1373-1387.
[19] Zhang J, Wang E, Zhang L and Zhou B. PSPH induces cell autophagy and promotes cell proliferation and invasion in the hepatocellular carcinoma cell line Huh7 via the AMPK/mTOR/ULK1 signaling pathway. Cell Biol Int 2021; 45: 305-319.
[20] Bachelor MA, Lu Y and Owens DM. L-3-Phosphoserine phosphatase (PSPH) regulates cutaneous squamous cell carcinoma proliferation independent of L-serine biosynthesis. J Dermatol Sci 2011; 63: 164-172.
[21] Yuan J, Dong X, Yap J and Hu J. The MAPK and AMPK signalings: interplay and implication in targeted cancer therapy. J Hematol Oncol 2020; 13: 113.
[22] DaSilva LL, Aguiar PN Jr and de Lima Lopes G. Immunotherapy for advanced esophageal squamous cell carcinoma-renewed enthusiasm and a lingering challenge. JAMA Oncol 2021; 7: 1613-1614.
[23] Chen Y, Yu R and Liu Y. Combine radiotherapy and immunotherapy in esophageal squamous cell carcinoma. Crit Rev Oncol Hematol 2023; 190: 104115.
[24] An L, Li M and Jia Q. Mechanisms of radiotherapy resistance and radiosensitization strategies for esophageal squamous cell carcinoma. Mol Cancer 2023; 22: 140.
[25] Vingeliene S, Chan DSM, Vieira AR, Polemiti E, Stevens C, Abar L, Navarro Rosenblatt D, Greenwood DC and Norat T. An update of the WCRF/AICR systematic literature review and meta-analysis on dietary and anthropometric

factors and esophageal cancer risk. Ann Oncol 2017; 28: 2409-2419.
[26] Ehlers CL, Benedict J, Wills D and Sanchez-Alavez M. PSPH-D-18-00526: effect of a dual orexin receptor antagonist (DORA-12) on sleep and event-related oscillations in rats exposed to ethanol vapor during adolescence. Psychopharmacology (Berl) 2020; 237: 2917-2927.
[27] Locasale JW. Serine, glycine and one-carbon units: cancer metabolism in full circle. Nat Rev Cancer 2013; 13: 572-583.
[28] Mattaini KR, Sullivan MR and Vander Heiden MG. The importance of serine metabolism in cancer. J Cell Biol 2016; 214: 249-257.
[29] Snell K, Natsumeda Y, Eble JN, Glover JL and Weber G. Enzymic imbalance in serine metabolism in human colon carcinoma and rat sarcoma. Br J Cancer 1988; 57: 87-90.
[30] Sayano T, Kawano Y, Kusada W, Arimoto Y, Esaki K, Hamano M, Udono M, Katakura Y, Ogawa T, Kato H, Hirabayashi Y and Furuya S. Adaptive response to l-serine deficiency is mediated by p38 MAPK activation via 1-deoxysphinganine in normal fibroblasts. FEBS Open Bio 2016; 6: 303-316.
[31] Ross KC, Andrews AJ, Marion CD, Yen TJ and Bhattacharjee V. Identification of the serine biosynthesis pathway as a critical component of BRAF inhibitor resistance of melanoma, pancreatic, and non-small cell lung cancer cells. Mol Cancer Ther 2017; 16: 1596-1609.
[32] Li X, Xun Z and Yang Y. Inhibition of phosphoserine phosphatase enhances the anticancer efficacy of 5-fluorouracil in colorectal cancer. Biochem Biophys Res Commun 2016; 477: 633-639.
[33] Lee S, Rauch J and Kolch W. Targeting MAPK signaling in cancer: mechanisms of drug resistance and sensitivity. Int J Mol Sci 2020; 21: 1102.
[34] Fang JY and Richardson BC. The MAPK signalling pathways and colorectal cancer. Lancet Oncol 2005; 6: 322-327.
[35] Colic E, Patel PU and Kent OA. Aberrant MAPK signaling offers therapeutic potential for treatment of ovarian carcinoma. Onco Targets Ther 2022; 15: 1331-1346.
[36] Ullah R, Yin Q, Snell AH and Wan L. RAF-MEK-ERK pathway in cancer evolution and treatment. Semin Cancer Biol 2022; 85: 123-154.
[37] Wagner EF and Nebreda AR. Signal integration by JNK and p38 MAPK pathways in cancer development. Nat Rev Cancer 2009; 9: 537-549.
[38] Iroegbu JD, Ijomone OK, Femi-Akinlosotu OM and Ijomone OM. ERK/MAPK signalling in the developing brain: perturbations and consequences. Neurosci Biobehav Rev 2021; 131: 792-805.
[39] Pua LJW, Mai CW, Chung FF, Khoo AS, Leong CO, Lim WM and Hii LW. Functional roles of JNK and p38 MAPK signaling in nasopharyngeal carcinoma. Int J Mol Sci 2022; 23: 1108.
[40] Delire B and Stärkel P. The Ras/MAPK pathway and hepatocarcinoma: pathogenesis and therapeutic implications. Eur J Clin Invest 2015; 45: 609-623.
[41] Lu M, Wang Y and Zhan X. The MAPK pathway-based drug therapeutic targets in pituitary adenomas. Front Endocrinol (Lausanne) 2019; 10: 330.
[42] Lee JJ, Jain V and Amaravadi RK. Clinical translation of combined MAPK and autophagy inhibition in RAS mutant cancer. Int J Mol Sci 2021; 22: 12402.
[43] Park HB and Baek KH. E3 ligases and deubiquitinating enzymes regulating the MAPK signaling pathway in cancers. Biochim Biophys Acta Rev Cancer 2022; 1877: 188736.
[44] Yong HY, Koh MS and Moon A. The p38 MAPK inhibitors for the treatment of inflammatory diseases and cancer. Expert Opin Investig Drugs 2009; 18: 1893-1905.
[45] Degirmenci U, Wang M and Hu J. Targeting aberrant RAS/RAF/MEK/ERK signaling for cancer therapy. Cells 2020; 9: 198.
[46] Ryan MB, Quade B, Schenk N, Fang Z, Zingg M, Cohen SE, Swalm BM, Li C, Özen A, Ye C, Ritorto MS, Huang X, Dar AC, Han Y, Hoeflich KP, Hale M and Hagel M. The Pan-RAF-MEK nondegrading molecular glue NST-628 is a potent and brain-penetrant inhibitor of the RAS-MAPK pathway with activity across diverse RAS- and RAF-driven cancers. Cancer Discov 2024; 14: 1190-1205.
[47] Subbiah V, Baik C and Kirkwood JM. Clinical development of BRAF plus MEK inhibitor combinations. Trends Cancer 2020; 6: 797-810.
[48] Zhou S, Ouyang W, Zhang X, Liao L, Pi X, Yang R, Mei B, Xu H, Xiang S and Li J. UTRN inhibits melanoma growth by suppressing p38 and JNK/c-Jun signaling pathways. Cancer Cell Int 2021; 21: 88.
[49] Ou S, Chen H, Wang H, Ye J, Liu H, Tao Y, Ran S, Mu X, Liu F, Zhu S, Luo K, Guan Z, Jin Y, Huang R, Song Y and Liu SL. Fusobacterium nucleatum upregulates MMP7 to promote metastasis-related characteristics of colorectal cancer cell via activating MAPK(JNK)-AP1 axis. J Transl Med 2023; 21: 704.
[50] Wu Q, Kuca K and Wu W. Targeting JNK and its role in tumor development and chemoresistance. Future Med Chem 2020; 12: 1103-1105.
[51] Bubici C and Papa S. JNK signalling in cancer: in need of new, smarter therapeutic targets. Br J Pharmacol 2014; 171: 24-37.

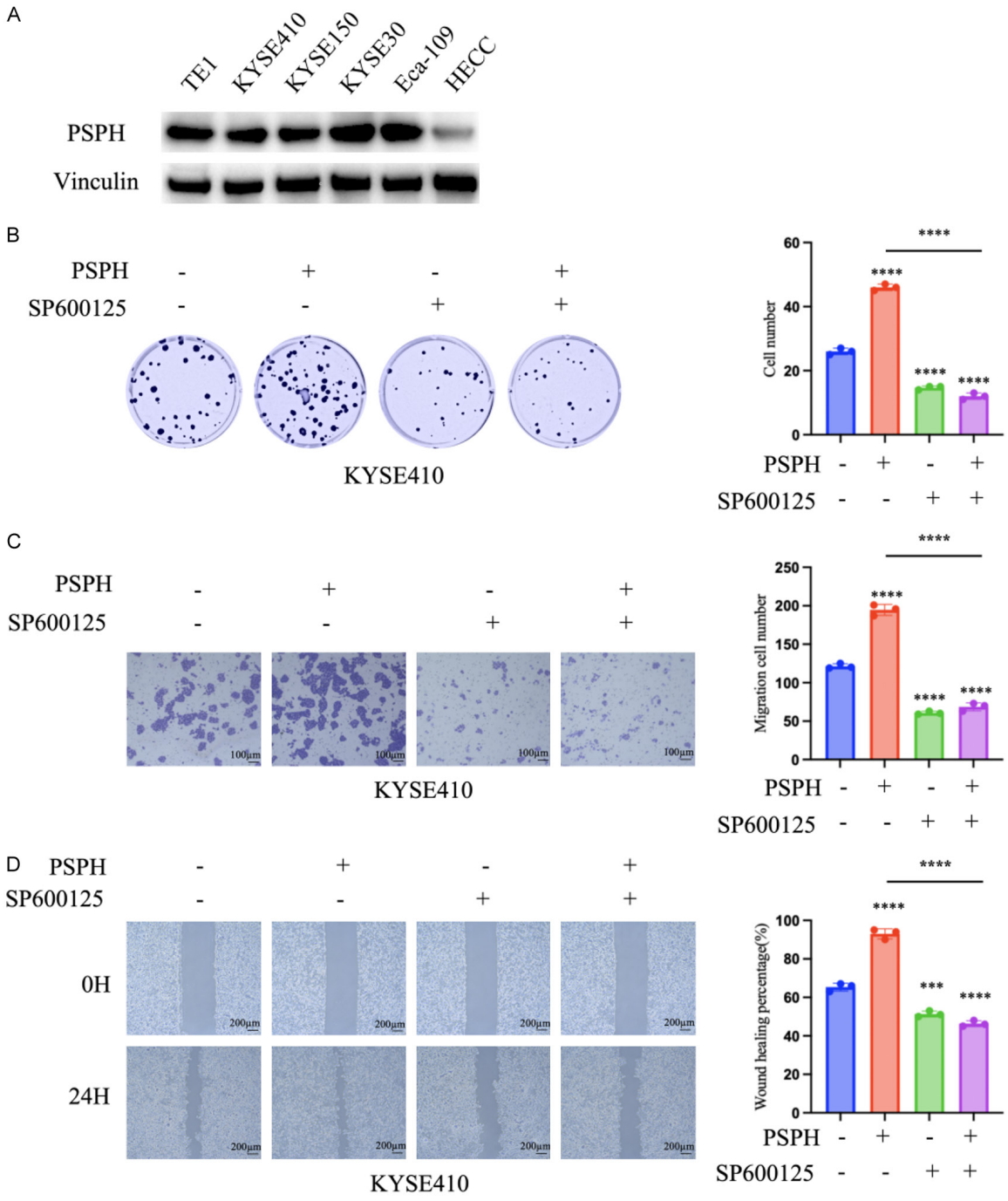

Figure S1. PSPH expression in esophageal cancer cell lines and rescue assay in KYSE410 cells. A. Western blot analysis of PSPH expression in five different esophageal cancer cell lines and one kind of normal esophageal cell (HECC). B. Colony formation of KYSE410 cells with PSPH overexpression treated with or without SP600125 (n=3). One-way ANOVA. ****P<0.0001. C. Migration assays in KYSE410 cells with PSPH overexpression treated with or without SP600125 (n=3). Scale bar: 100 μm. One-way ANOVA. ****P<0.0001. D. Wound healing assay of KYSE410 cells with PSPH overexpression treated with or without SP600125 (n=3). Scale bar: 200 μm. One-way ANOVA. ***P<0.001, ****P<0.0001.